

# UC Berkeley

## UC Berkeley Previously Published Works

### Title

A  $\beta$ -Peptide Agonist of the GLP-1 Receptor, a Class B GPCR

### Permalink

<https://escholarship.org/uc/item/4k04t2t1>

### Journal

Organic Letters, 15(20)

### ISSN

1523-7060

### Authors

Denton, Elizabeth V  
Craig, Cody J  
Pongratz, Rebecca L  
[et al.](#)

### Publication Date

2013-10-18

### DOI

10.1021/ol402568j

Peer reviewed

Published in final edited form as:

Org Lett. 2013 October 18; 15(20): 5318–5321. doi:10.1021/ol402568j.

## A $\beta$ -peptide agonist of the GLP-1 receptor, a class B GPCR

Elizabeth V. Denton<sup>†</sup>, Cody J. Craig<sup>†</sup>, Rebecca L. Pongratz<sup>‡</sup>, Jacob S. Appelbaum<sup>§</sup>, Amy E. Doerner<sup>†</sup>, Arjun Narayanan<sup>†</sup>, Gerald I. Shulman<sup>‡,||,⊥</sup>, Gary W. Cline<sup>‡</sup>, and Alanna Schepartz<sup>\*,†,#</sup>

<sup>†</sup>Department of Chemistry, Yale University

<sup>‡</sup>Department of Internal Medicine, Yale University School of Medicine

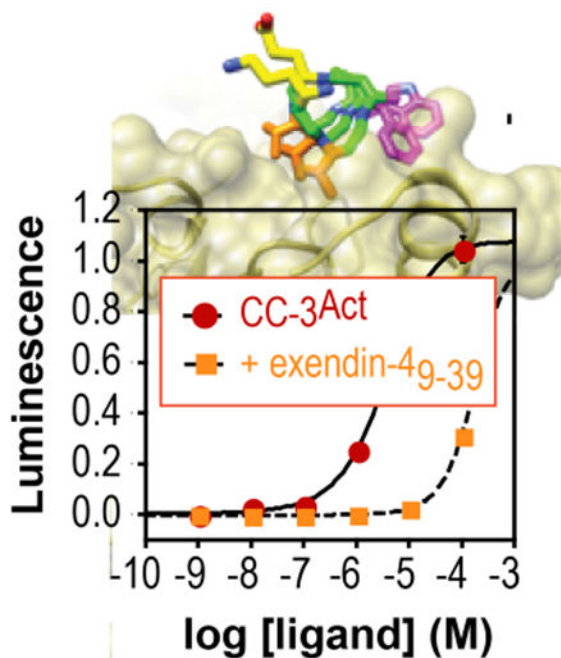
<sup>§</sup>Department of Cell Biology, Yale University School of Medicine

<sup>||</sup>Department of Cellular and Molecular Physiology, Yale University School of Medicine

<sup>⊥</sup>Howard Hughes Medical Institute, Yale University School of Medicine

<sup>#</sup>Department of Molecular, Cellular and Developmental Biology, Yale University

### Abstract



Previous work has shown that certain  $\beta^3$ -peptides can effectively mimic the side chain display of an  $\alpha$ -helix and inhibit interactions between proteins, both *in vitro* and in cultured cells. Here we describe a  $\beta^3$ -peptide analog of GLP-1, CC-3<sup>Act</sup>, that interacts with the GLP-1R extracellular

Correspondence to [alanna.schepartz@yale.edu](mailto:alanna.schepartz@yale.edu).

**Supporting Information Available.** Peptide synthesis and characterization, assay procedures, and supplemental figures.

domain (nGLP-1R) *in vitro* in a manner that competes with exendin-4 and induces GLP-1R-dependent cAMP signaling in cultured CHO-K1 cells expressing GLP-1R.

The primary role of pancreatic  $\beta$  cells is to synthesize and secrete insulin. This function is modulated in part by a set of heterotrimeric G proteins that are the immediate downstream targets of diverse G protein-coupled receptors (GPCRs). A number of GPCRs expressed by pancreatic  $\beta$  cells regulate insulin secretion. One, the receptor for the glucagon-like peptide-1 (GLP-1R), binds to and is activated by glucagon-like peptide-1 (GLP-1),<sup>1, 2</sup> a 30-aa member of the incretin hormone family. In the presence of glucose, activated GLP-1R signals through the associated G protein  $G_s$  to activate the adenylyl cyclase pathway and stimulate insulin secretion.<sup>3</sup> Indeed, GLP-1R is a validated target for the treatment of type 2 diabetes mellitus.<sup>3, 4</sup> Exendin-4, a 39-aa GLP-1 ortholog<sup>5</sup> possessing improved serum stability, was approved for use in 2005. Additional GLP-1 mimetics with improved pharmacodynamics are in development,<sup>6, 7</sup> and efforts have begun to identify low molecular weight compounds that may allow oral administration.<sup>8-15</sup> Furthermore, new bi-functional peptides that activate GLP-1R and other molecular targets are being explored in pre-clinical models for enhanced anti-diabetic pharmacology.<sup>16, 17</sup>

Previous work has shown that certain  $\beta^3$ -peptides can effectively mimic the side chain display of an  $\alpha$ -helix and inhibit interactions between proteins, both *in vitro*<sup>18-20</sup> and in cultured cells.<sup>21-23</sup> Oligomers containing mixtures of both  $\alpha$ - and  $\beta$ -amino acids have also shown success.<sup>24</sup> Here we describe a potential  $\beta^3$ -peptide analog of GLP-1, CC-3<sup>Act</sup>, that interacts with the GLP-1R extracellular domain (nGLP-1R) *in vitro* in a manner that competes with exendin-4 and induces GLP-1R-dependent cAMP signaling in cultured CHO-K1 cells expressing GLP-1R.

Our design of CC-3<sup>Act</sup> began with the sequence of exendin-4. This sequence can be divided into two regions: a 22 residue C-terminal region that associates as an  $\alpha$ -helix (shown in purple in Figure 1) with nGLP-1R (shown in grey) and functions in isolation as a receptor antagonist ( $K_d = 5$  nM<sup>5</sup>) and an 9 residue N-terminal region of undefined structure that is required for receptor activation.<sup>5, 25, 26</sup> A large number side chains within the C-terminal region contribute to exendin-4/GLP-1R binding and/or receptor activation; these include E<sub>15</sub>, F<sub>22</sub>, I<sub>23</sub>, and L<sub>26</sub>; modest contributions are also made by L<sub>14</sub>, K<sub>20</sub>, A<sub>24</sub>, W<sub>25</sub>, V<sub>27</sub> and K<sub>28</sub>. Of these side chains, five–A<sub>18</sub>, W<sub>25</sub>, F<sub>22</sub>, L<sub>26</sub>, and A/V<sub>19</sub>–are conserved between exendin-4 and GLP-1 and localize on the bound  $\alpha$ -helix at the ligand-receptor interface (Figure 1C).<sup>27</sup>

Our design was further refined by three principles uncovered during previous efforts to develop  $\beta^3$ -peptide mimics of less complex  $\alpha$ -helical segments.<sup>18, 20-23, 28, 29</sup> These efforts revealed that homo-oligomeric  $\beta^3$ -peptides presenting three interacting residues on one 14-helix face often perform as designed, binding their targets with affinities  $< 1$   $\mu$ M, whereas those presenting four interacting residues usually do not. These efforts also revealed that the axial orientation of the three interacting residues (N to C vs. C to N) and their stereochemical relationship (Figure 1D) could modulate  $K_d$  by more than 100-fold. The side chain that contributes most significantly to exendin-4•GLP-1R interaction is F<sub>22</sub>.<sup>30</sup> Thus, we began by identifying a collection of side chain triads containing F<sub>22</sub> and other components

of the bound  $\alpha$ -helix interface that could be displayed on each of two 14-helix faces and in either the N to C or C to N direction. For example, were F<sub>22</sub> to occupy position *d* of a heptad repeat, the *ada* side chain triad would include V<sub>19</sub>, F<sub>22</sub>, and L<sub>26</sub>; were it to occupy position *a*, the *dad* triad would be A<sub>18</sub>, F<sub>22</sub>, and W<sub>25</sub>. Each of these three residue epitopes can be presented in two axial directions and on two 14-helix faces to generate a collection of 8  $\beta^3$ -peptides.  $\beta^3$ -peptides presenting VFW and AFL epitopes (formally *adg* and *gda*) were also prepared to generate a collection of 16 molecules (Figure 1E).

First we used an *in vitro* fluorescence polarization (FP) competition assay to compare the relative affinities of these 16  $\beta^3$ -peptides for recombinant nGLP-1R (Figure S1). Each  $\beta^3$ -peptide was incubated at a concentration of 10 or 50  $\mu\text{M}$  with 5 nM exendin-4<sup>Flu</sup> in the presence of 125 nM nGLP-1R, and the polarization of the mixture was monitored at equilibrium. Fourteen of the sixteen  $\beta^3$ -peptides evaluated had no effect on the observed polarization, even at 50  $\mu\text{M}$  concentration, indicating that they had little or no effect on the fraction of exendin-4<sup>Flu</sup> bound to the nGLP-1R under these conditions.  $\beta^3$ -peptides CC-3 and CC-11, however, both significantly reduced the observed polarization values (22 and 33% relative to exendin-4), suggesting that they compete with exendin-4<sup>Flu</sup> for the nGLP-1R binding pocket. Incubation of 5 nM exendin-4<sup>Flu</sup> and 125 nM nGLP-1R with between 10 nM and 500  $\mu\text{M}$  CC-3 or CC-11 led to a concentration-dependent decrease in the fraction of exendin-4<sup>Flu</sup> bound (Figure 2A); subsequent data analysis suggested IC<sub>50</sub> (and *K<sub>i</sub>*) values of  $228 \pm 35 \mu\text{M}$  ( $115 \pm 18$ ) and  $116 \pm 31$  ( $84 \pm 16$ )  $\mu\text{M}$  for CC-3 and CC-11, respectively. In comparison, the  $\alpha$ -peptide antagonist GLP-1<sub>15-37</sub> was only 15-20 times more potent than CC-11 in this assay, competing with exendin-4<sup>Flu</sup> with IC<sub>50</sub> and *K<sub>i</sub>* values of  $7.53 \pm 0.54$  and  $3.75 \pm 0.23 \mu\text{M}$  respectively. Differences between exendin-4 and GLP-1 binding to the GLP-1R ectodomain *in vitro* are well described.<sup>31</sup> Even the modest affinity of GLP-1 for nGLP-1R is sufficient for subnanomolar potency in the context of the full-length receptor and peptide.

Three lines of evidence suggest that CC-3 and CC-11 mimic the  $\alpha$ -helical regions of exendin-4 and GLP-1 in their interactions with nGLP-1R. First, substitution of each component of the 'AFW/VFW' epitope for alanine (CC-3.6, CC-3.9) or ornithine (CC-3.3) led to ( $\beta^3$ -peptides that compete poorly with exendin-4<sup>Flu</sup> for binding to nGLP-1R (Figure 2B). Second, CC-3 and CC-11 differ by only two methyl groups, presenting either an AFW (CC-3) or VFW (CC-11) triad in the N-to-C orientation on the same  $\beta^3$ -peptide face. Six other collection members carry one of these two side chain triads (CC-1, 2, and 4; CC-9, 10, 12), but differ from CC-3 and CC-11 in the relative orientation of the three side chains (N-to-C or C-to-N) or the stereochemical relationship of the epitope, hydrophobic, and salt bridge faces. Yet, only CC-3 and CC-11 competed effectively with exendin-4<sup>Flu</sup> for binding to nGLP-1R (Figure 2B).

Finally, *post hoc* modeling experiments provide a structural rationale for the observed differences in affinity among  $\beta^3$ -peptides possessing alternate arrangements of the same binding epitope. We used the program *pepz*<sup>32</sup> to construct models for ( $\beta^3$ -peptides CC-1-4 and CC-9-12 in an ideal 3<sub>14</sub>-helix conformation.<sup>33</sup> After sampling of the epitope side-chains, the C $\beta$ , C $\gamma$ , C $\delta$ , C $\epsilon$ 1 and N $\zeta$ 1 atoms of the epitope residues were used to align each  $\beta^3$ -peptide to the corresponding side chain atoms (C $\beta$ , C $\gamma$ , C $\delta$ , C $\epsilon$ 1 and N $\zeta$ 1) of exendin-4

in the exendin-4•nGLP-R complex structure (PDBID 3c5t). The RMSD of these alignments varied between 1.1-1.4 Å (shown in Figure S2). While these models are too coarse to reveal detailed interactions or the precise placement of each side chain in the binding pocket, they do identify the relative orientation of side chains presented on each  $3_{14}$  helix face. In the case of CC-3 and CC-11, alignment of the AFW/VFW epitopes into the binding pocket orients the ( $\beta^3$ -peptide hydrophobic face, which contains three valine side chains, towards a hydrophobic groove on the GLP-1R surface, and orients the salt-bridge face, which contains acidic and basic side chains, towards solvent. Reversing the C-to-N direction of the AFW/VFW epitope as in CC-1 and CC-9, or reversing the relative orientation of the salt-bridge and valine faces with respect to the epitope face as in CC-4 and CC-12, directs the salt-bridge face towards the hydrophobic groove on the nGLP-1R surface and points the hydrophobic valine side-chains towards solvent. These two side chain arrangements are likely to be energetically unfavorable and destabilize the interaction of these  $\beta^3$ -peptides with nGLP-1R. Interestingly, reversal of *both* the face ordering and the N-to-C directionality (as in CC-2 and CC-10) leads to side-chain placement similar to that of CC-3 and CC-11. In this case, the reduced  $3_{14}$  helicity of CC-2 and CC-10 may be the primary cause for their reduced binding (Figure S3).

Next, CC-3 and CC-11 were converted into the potential ( $\beta^3$ -hormones CC-3<sup>Act</sup> and CC-11<sup>Act</sup>) by extending their sequence at the N-terminus with a 13-atom polyethylene glycol (PEG) chain followed by the  $\alpha$ -peptide NH<sub>2</sub>-HGEFTFTSD, which corresponds to the nine N-terminal residues of exendin-4 and are critical for GLP-1R activation<sup>30</sup> (Figure 1). Procedures to minimize aspartimide formation<sup>34</sup> were employed and validated<sup>35,36</sup> and the products were purified using pristine HPLC columns to avoid cross-contamination with GLP-1 itself. Ligand-dependent GPCR activation was monitored in GLP-1R+ CHO-K1 cells using a luciferase reporter gene under control of a cAMP response element promoter.<sup>30</sup> As expected, GLP-1 was a potent GLP-1R agonist ( $EC_{50} = 2.86 \pm 0.70$  pM), and was inhibited by 1  $\mu$ M exendin-4<sub>9-39</sub>, CC-3 or CC-11, in accord with the relative *in vitro* affinities of these ligands (Figure 3A). Both CC-3<sup>Act</sup> and CC-11<sup>Act</sup> activated GLP-1R in CHO-K1 cells ( $EC_{50} = 1.2 \pm 0.74$   $\mu$ M and  $13.2 \pm 2.5$   $\mu$ M respectively (Figure 3B). Activation of GLP-1R by CC-3<sup>Act</sup> was reduced 50-fold by 1  $\mu$ M exendin-4<sub>9-39</sub> (Figure 3C), suggesting that the observed increase in cAMP resulted from a direct interaction of CC-3<sup>Act</sup> with the GLP-1R ligand-binding domain. In addition, loss of any of the three side chains that contributed to receptor affinity *in vitro* (Figures 1 and 2) decreased potency in the cell based assay (Figure 3D). Finally, an analog of CC-3<sup>Act</sup> lacking a PEG linker (CC-3<sup>Act-1</sup>) was inactive (Figure 3D), consistent with the need for a discrete structural relationship between the C- and N-terminal domains.

GLP-1R is one of several homologous class B1 GPCRs expressed in the pancreas. Other family members include the receptors activated by peptides known as GIP, glucagon, VIP, and PACAP.<sup>37-39</sup> To investigate the selectivity of CC-3<sup>Act</sup> as a GLP-1R agonist, we examined its effect on the activation of these four receptors in CHO-K1 cells. Although each of these receptors were activated potently by their cognate ligands (Figure 3E), none were activated by CC-3<sup>Act</sup> (or CC-11<sup>Act</sup>), even at high concentration (Figure 3F).

Although the results reported herein suggest that CC-3<sup>Act</sup> activates GLP-1R through interactions that mimic those of GLP-1 and exendin-4, its potency was modest—a full six orders of magnitude lower than GLP-1. Even mM concentrations of CC-3<sup>Act</sup> did not inhibit forskolin-dependent activation of the adenylate cyclase pathway (Figure S4), ruling out the possibility that the lower-than-expected potency of CC-3<sup>Act</sup> was due to unexpected interference with a later step in the activation pathway. We note, however, that the high *in vitro* potencies of GLP-1 and orthologs are counterbalanced by the rapid elimination and short half-lives of the peptides *in vivo*.  $\beta^3$ -peptides are not subject to the same degradation processes and all available studies indicate dramatically enhanced stability *in vivo*.<sup>40-43</sup> Further optimization of these sequences is ongoing in our laboratory.

## Supplementary Material

Refer to Web version on PubMed Central for supplementary material.

## Acknowledgments

We are grateful to the National Institutes of Health for support of this work.

## References

1. Thorens B. Proc Natl Acad Sci USA. 1992; 89:8641–8645. [PubMed: 1326760]
2. Dillon JS, Tanizawa Y, Wheeler MB, Leng XH, Ligon BB, Rabin DU, Yoo-Warren H, Permutt MA, Boyd AE. Endocrinology. 1993; 133:1907–1910. [PubMed: 8404634]
3. Drucker DJ. Cell Metab. 2006; 3:153–165. [PubMed: 16517403]
4. Lovshin JA, Drucker DJ. Nat Rev Endocrinol. 2009; 5:262–269. [PubMed: 19444259]
5. Goke R, Fehmann HC, Linn T, Schmidt H, Krause M, Eng J, Goke B. J Biol Chem. 1993; 268:19650–19655. [PubMed: 8396143]
6. Garber AJ. Expert Opin Investig Drugs. 2012; 21:45–57.
7. Madsbad S, Kielgast U, Asmar M, Deacon CF, Torekov SS, Holst JJ. Diabetes Obes Metab. 2011; 13:394–407. [PubMed: 21208359]
8. Willard FS, Bueno AB, Sloop KW. Exp Diabetes Res. 2012; 2012:709893–709893. [PubMed: 22611375]
9. Wootten D, Savage EE, Willard FS, Bueno AB, Sloop KW, Christopoulos A, Sexton PM. Mol Pharm. 2013; 83:822–834.
10. Eng H, Sharma R, McDonald TS, Edmonds DJ, Fortin JP, Li X, Stevens BD, Griffith DA, Limberakis C, Nolte WM, Price DA, Jackson M, Kalgutkar AS. Drug Metab Dis. 2013; 41:1470–1479.
11. Willard FS, Wootten D, Showalter AD, Savage EE, Ficorilli J, Farb TB, Bokvist K, Alsina-Fernandez J, Furness SGB, Christopoulos A, Sexton PM, Sloop KW. Mol Pharm. 2012; 82:1066–1073.
12. Li N, Lu J, Willars GB. Plos One. 2012; 7
13. He M, Guan N, Gao Ww, Liu Q, Wu Xy, Ma Dw, Zhong Df, Ge Gb, Li C, Chen Xy, Yang L, Liao Jy, Wang Mw. Acta Pharm Sinica. 2012; 33:148–154.
14. Gong YD, Cheon HG, Lee T, Kang NS. Bull Korean Chem Soc. 2010; 31:3760–3764.
15. Mapelli C, Natarajan SI, Meyer JP, Bastos MM, Bernatowicz MS, Lee VG, Pluscec J, Riexinger DJ, Sieber-McMaster ES, Constantine KL, Smith-Monroy CA, Golla R, Ma Z, Longhi DA, Shi D, Xin L, Taylor JR, Koplowitz B, Chi CL, Khanna A, Robinson GW, Seethala R, Anatal-Zimanyi IA, Stoffel RH, Han S, Whaley JM, Huang CS, Krupinski J, Ewing WR. J Med Chem. 2009; 52:7788–7799. [PubMed: 19702274]

16. Day JW, Ottaway N, Patterson JT, Gelfanov V, Smiley D, Gidda J, Findeisen H, Bruemmer D, Drucker DJ, Chaudhary N, Holland J, Hembree J, Abplanalp W, Grant E, Ruehl J, Wilson H, Kirchner H, Lockie SH, Hofmann S, Woods SC, Nogueiras R, Pfluger PT, Perez-Tilve D, DiMarchi R, Tschop MH. *Nat Chem Biol*. 2009; 5:749–757. [PubMed: 19597507]
17. Tschop MH, DiMarchi RD. *Diabetes*. 2012; 61:1309–1314. [PubMed: 22618765]
18. Kritzer JA, Lear JD, Hodsdon ME, Schepartz A. *J Am Chem Soc*. 2004; 126:9468–9469. [PubMed: 15291512]
19. Michel J, Harker EA, Tirado-Rives J, Jorgensen WL, Schepartz A. *J Am Chem Soc*. 2009; 131:6356–6357. [PubMed: 19415930]
20. Bautista AD, Appelbaum JS, Craig CJ, Michel J, Schepartz A. *J Am Chem Soc*. 2010; 132:2904–2906. [PubMed: 20158215]
21. Stephens OM, Kim S, Welch BD, Hodsdon ME, Kay MS, Schepartz A. *J Am Chem Soc*. 2005; 127:13126–13127. [PubMed: 16173723]
22. Bautista AD, Stephens OM, Wang L, Domaol RA, Anderson KS, Schepartz A. *Bioorg Med Chem Lett*. 2009; 19:3736–3738. [PubMed: 19497744]
23. Harker EA, Daniels DS, Guarracino DA, Schepartz A. *Bioorg Med Chem*. 2009; 17:2038–2046. [PubMed: 19211253]
24. Lee EF, Smith BJ, Horne WS, Mayer KN, Evangelista M, Colman PM, Gellman SH, Fairlie WD. *ChemBioChem*. 2011; 12:2025–2032. [PubMed: 21744457]
25. Mann R, Nasr N, Hadden D, Sinfield J, Abidi F, Al-Sabah S, de Maturana RL, Treece-Birch J, Willshaw A, Donnelly D. *Biochem Soc Trans*. 2007; 35:713–716. [PubMed: 17635131]
26. Al-Sabah S, Donnelly D. *Br J Pharmacol*. 2003; 140:339–346. [PubMed: 12970080]
27. Runge S, Thogersen H, Madsen K, Lau J, Rudolph R. *J Biol Chem*. 2008; 283:11340–11347. [PubMed: 18287102]
28. Kritzer JA, Hodsdon ME, Schepartz A. *J Am Chem Soc*. 2005; 127:4118–4119. [PubMed: 15783163]
29. Kritzer JA, Stephens OM, Guarracino DA, Reznik SK, Schepartz A. *Bioorganic & Medicinal Chemistry*. 2005; 13:11–6. [PubMed: 15582447]
30. Adelhorst K, Hedegaard BB, Knudsen LB, Kirk O. *J Biol Chem*. 1994; 269:6275–6278. [PubMed: 8119974]
31. Willard FS, Sloop KW. *Exp Diabetes Res*. 2012; 2012:470851–470851. [PubMed: 22666230]
32. Jorgensen WL, Tirado-Rives J. *J Comp Chem*. 2005; 26:1689–1700. [PubMed: 16200637]
33. DeGrado WF, Schneider JP, Hamuro Y. *Chem Biol Drug Des*. 1999; 54:206–217.
34. Subiros-Funosas R, El-Faham A, Albericio F. *Tetrahedron*. 2011; 67:8595–8606.
35. Kameoka D, Ueda T, Imoto T. *J Biochem*. 2003; 134:129–135. [PubMed: 12944379]
36. Ni W, Dai S, Karger BL, Zhou ZS. *Anal Chem*. 2010; 82:7485–7491. [PubMed: 20712325]
37. Ahren B. *Nat Rev Drug Discov*. 2009; 8:369–385. [PubMed: 19365392]
38. Regard JB, Kataoka H, Cano DA, Camerer E, Yin L, Zheng YW, Scanlan TS, Hebrok M, Coughlin SR. *J Clin Inv*. 2007; 117:4034–4043.
39. Winzell MS, Ahren B. *Peptides*. 2007; 28:1805–1813. [PubMed: 17559974]
40. Hintermann T, Seebach D. *CHIMIA*. 1997; 51:244–247.
41. Hook DF, Bindschadler P, Mahajan YR, Sebesta R, Kast P, Seebach D. *Chem Biodiversity*. 2005; 2:591–632.
42. Seebach D, Abele S, Schreiber JVJ, Martinoni B, Nussbaum AK, Schild H, Schulz H, Hennecke H, Woessner R, Bitsch F. *CHIMIA*. 1998; 52:734–739.
43. Seebach D, Overhand M, Kühnle FNM, Martinoni B, Oberer L, Hommel U, Widmer H. *Helv Chim Acta*. 1996; 79:913–941.

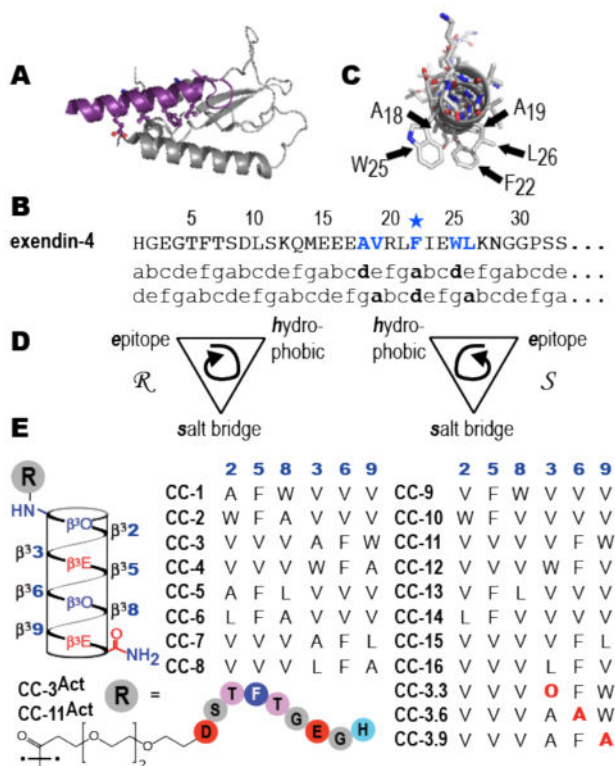


**Figure 1.**

(A) View of exendin-4 (purple) in complex with nGLP-1R (grey) (PDB 3C5T) illustrating relative orientation of the incretin  $\alpha$ -helix and the Sushi fold of the receptor extracellular domain. (B) Sequence of exendin-4 aligned with two heptad repeats. (C) View of GLP-1 looking down the helix axis to illustrate side chain arrangement at the ligand-receptor interaction face. (D) Cartoon illustrating the stereochemical relationships between the three 14-helix faces. (E) Helical net and sequences of  $\beta$ -peptides evaluated herein.



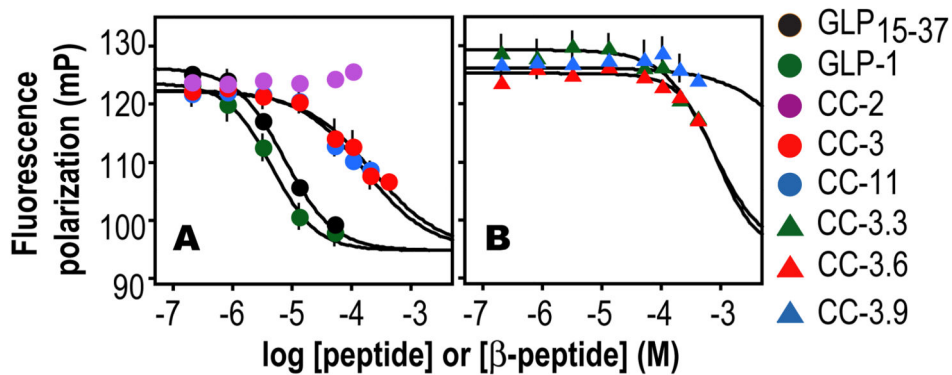
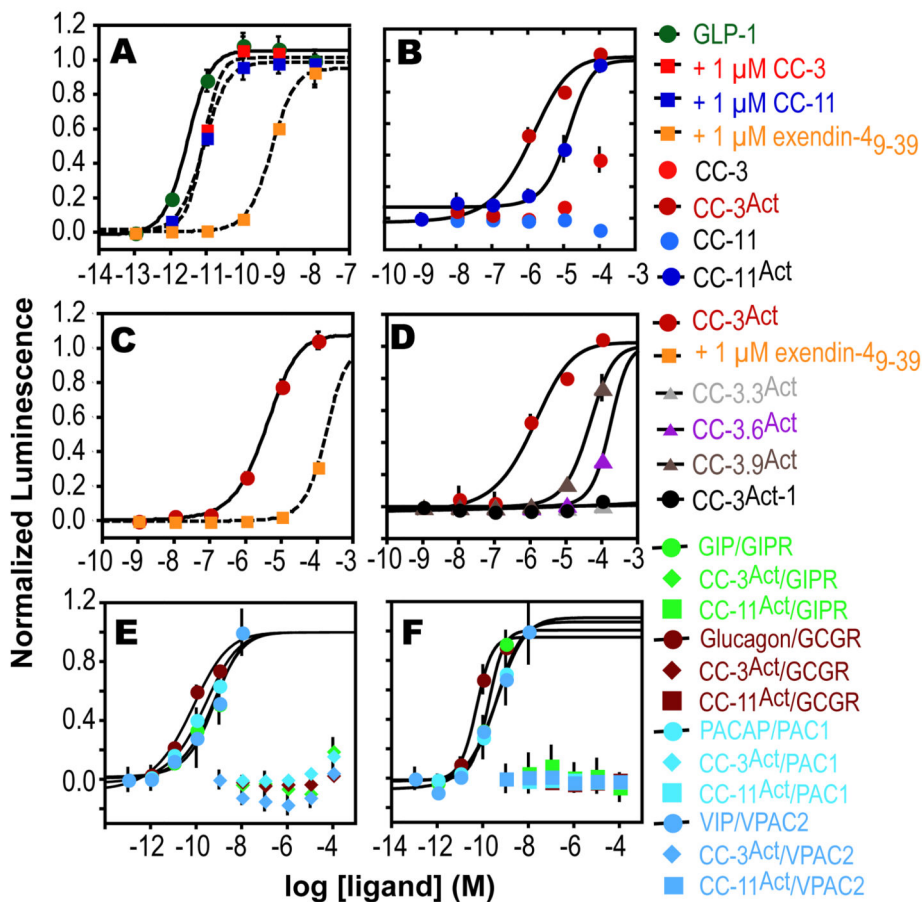


Figure 2.

Fluorescence polarization (FP) competition analysis of interactions between nGLP-1R and either peptides (GLP-1 and GLP1<sub>5-37</sub>) or  $\beta^3$ -peptides. Plots illustrate the change in the polarization of 5 nM extendin-4<sup>Flu</sup> as a function of the concentration of the ligand indicated; [nGLP-1R] = 125 nM.



**Figure 3.**

Effect of  $\beta$ -peptides and ligands on cAMP production in cells expressing class B1 GPCRs. (A-D) Effect of various  $\beta$ -peptides and exendin-4 on cAMP accumulation in GLP-1R+ CHO-K1 cells. (E,F) cAMP accumulation in GIPR+, PAC1+, GCCR+, and VPAC+CHO-K1 cells upon treatment with the cognate ligand, CC-3<sup>Act</sup> or CC-11<sup>Act</sup>.